ESTIMATING THE SOLAR ACCESS OF TYPICAL RESIDENTIAL ROOFTOPS: A CASE STUDY IN SAN JOSE, CA

Ronnen Levinson
Hashem Akbari
Melvin Pomerantz
Heat Island Group, Lawrence Berkeley National Lab
1 Cyclotron Road, MS 90R2000
Berkeley, CA 94720
e-mail: RML27@cornell.edu
e-mail: H_Akbari@LBL.gov
e-mail: M_Pomerantz@LBL.gov

Smita Gupta
California Energy Commission
1516 Ninth St. MS 42
Sacramento, CA 95814
e-mail: Sgupta@energy.state.ca.us

ABSTRACT

Shadows cast by trees and buildings can limit the solar access of rooftop solar-energy systems, including photovoltaic panels and thermal collectors. This study characterizes rooftop shading in a residential neighborhood of San Jose, CA, one of four regions analyzed in a wider study of the solar access of California homes.

High-resolution orthophotos and LiDAR (Light Detection And Ranging) measurements of surface height were used to create a digital elevation model of all trees and buildings in a 4 km^2 residential neighborhood. Hourly shading of roofing planes (the flat elements of roofs) was computed geometrically from the digital elevation model. Parcel boundaries were used to determine the extent to which roofing planes were shaded by trees and buildings in neighboring parcels.

In the year in which surface heights were measured (2005), shadows from all sources ("total shading") reduced the insolation received by S-, SW-, and W-facing residential roofing planes in the study area by 13 – 16%. Shadows cast by trees and buildings in neighboring parcels reduced insolation by no more than 2%. After 30 years of simulated maximal tree growth, annual total shading increased to 19 – 22%, and annual extraparcel shading increased to 3 – 4%.

1. INTRODUCTION

Tree-planting programs designed to shade and cool the south or west sides of buildings can inadvertently limit the solar access of rooftop solar-energy systems, including photovoltaic panels and thermal collectors.

Several researchers have modeled the influence of shade on the solar access of buildings. Kaye et al. [1] observed from the street the geometries of the roofs on and trees near 60 houses in an inner-city suburban region of Sydney, Australia. They then used ray-tracing software to predict the locations of hourly shadows and estimate the average daily output of a nominally 1 kW rooftop photovoltaic array during winter months. Mardaljavec and Rylatt [2] applied the *Radiance* lighting-simulation system to a three-dimensional model of San Francisco to generate a map of annual insolation on modeled urban surfaces, including walls and roofs. Compagnon [3] also applied *Radiance* to three-dimensional building models to estimate urban solar availability, but presented results only for walls.

The CH2MHill Solar Automated Feature Extraction™ methodology [4] uses stereo aerial imagery to build three-dimensional model of buildings, then geometrically computes each building's solar access. The current version of this software (winter 2008) does not consider trees because it is difficult to determine the heights of curved surfaces from stereo imagery.

Simpson [5] and Akbari [6] each modeled the influence of tree shading on residential energy use for heating and cooling. McPherson and Simpson [7] determined tree-canopy coverage from aerial photographs of 21 California cities to determine the extent to which tree planting programs could reduce energy use in California communities. Akbari et al. [8] and Rose et al. [9] also estimated urban tree cover from high-resolution orthophotos. However, none of these studies quantified shading of rooftops.

This paper estimates the extent to which shading reduces the solar radiation incident on residential roofs in San Jose as

part of a larger effort to gauge the influence of shading on residential rooftop solar access in various California cities, including Sacramento, San Jose, Los Angeles, and San Diego. This shading analysis can be used to better estimate power production and/or thermal collection by rooftop solar-energy equipment. It can also be considered when designing programs to plant shade trees.

2. METHODOLOGY

The locations and elevation profiles of buildings and trees were estimated by combining aerial photography with remote measurements of surface height. The fraction of each flat element of the roof's surface, or "roofing plane," that is shaded at a given hour of the year was determined by geometric computation of the extent to which trees and buildings obscure the path between the sun and the plane. The light loss (loss of incident solar power/area) at any given hour is the product of this shade fraction and the insolation on an unshaded surface of like orientation. Annual shading, or the fraction by which shading reduces the annual insolation received by a roofing plane, is the ratio of annual light loss to annual insolation in the absence of shading.

Shading in future years is estimated by repeating these calculations after simulating tree growth.

2.1 Spatial Data Selection

A well-treed residential neighborhood in San Jose, CA containing a mix of single- and double-story tract homes built between 1980 and 1990 was selected. This provided a study region in which trees were about 20 years old in 2005, and thus tall enough to shade the roofs of these typical modern homes (Fig. 1).

2.2 Spatial Data Acquisition

High-resolution digital color orthophotos and LiDAR (Light Detection And Ranging) measurements of surface elevation (height above sea level versus easting and northing) were collected by airplane-mounted instruments. Orthophoto pixel resolution was 7.6 cm (3 in). The horizontal spacing of LiDAR points was 140 cm, with a horizontal accuracy of 46 cm and a vertical accuracy of 36 cm. A detail of a San Jose orthophoto is shown in Fig. 2.

2.3 Shading Analysis

The following analysis employed the ESRI ArcView 9.1 geographic information system (GIS) tool [10].

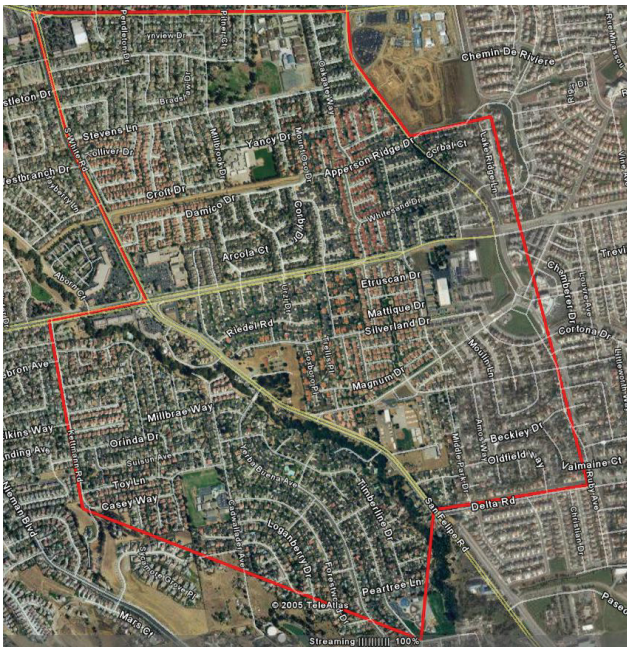

Fig. 1: Aerial view of 4.1 km^2 study area in San Jose, CA (red polygon).

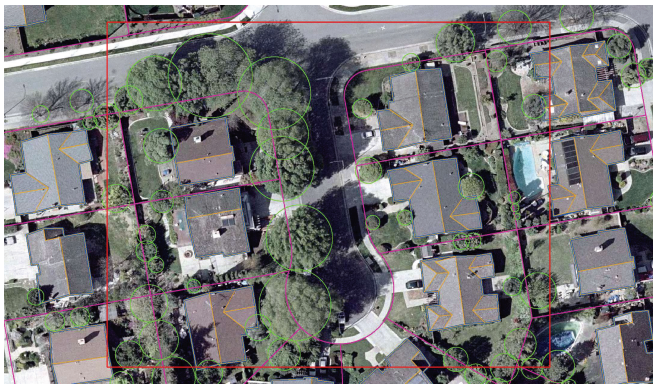

Fig. 2: Roof (blue), plane (gold), tree (green) and parcel (magenta) shapes overlaid on detail of orthophoto.

2.3.1 Roof, Plane, Trees, and Parcel Outlines

The shapes (ground-plane projection outlines) of all roofs, planes, and tree canopies were manually traced from high resolution color orthophotos rendered in the GIS tool, while parcel shapes were acquired from the city of San Jose.

2.3.2 Elevation and Height Rasters

The year of the LiDAR survey (2005) is denoted year zero. A year-zero raster of surface elevation (surface height above sea level) spanning the study region was computed via inverse-distance-weighted interpolation of the LiDAR

surface elevation measurements (Fig. 3). All generated rasters contain square cells 50 cm on a side.

A ground-elevation raster (ground height above sea level) was computed as the 50-m focal minimum of the surface-elevation raster, and the surface-height raster (surface height above ground) was computed by subtracting the ground-elevation raster from the surface-elevation raster. Finally, the study-region surface-elevation raster was disaggregated by parcel to create a set of several thousand "parcel" surface-elevation rasters.

Additional rasters of surface elevation were constructed to account for tree growth after 10, 20 and 30 years. Tree height h at age t was approximated with the asymptotic growth model

$$h(t) = H\left[1 - \exp(-t/\tau)\right], \qquad (1)$$

where H is the mature height of the tree. In this model, the time constant τ, or age at which the tree reaches about 63% of its mature height, is equal to the ratio of the tree's mature height H to its initial growth rate. Tree-canopy width was not increased over time in our analysis.

If the height of the tree at age t_0 is known to be h_o, the time constant τ can be eliminated from Eq. (1) to yield

$$h(t) = H\left[1 - \left(1 - h_0/H\right)^{t/t_0}\right]. \qquad (2)$$

Assuming that all trees were planted when the homes were built made them about 20 years old in year zero. Each tree's height at this age was estimated as the maximum year-zero surface height-above-ground of cells within its traced border. An upper-limit to future-year shading was estimated with Eq. (2) by applying to all trees the mature height associated with the tallest species of trees found in the study regions (H = 20 m).

Future-year rasters of surface height above ground were generated by "growing" the trees in the year-zero raster of surface height above ground. Future-year surface elevation (above sea level) was then calculated by adding future-year surface height above ground to year-zero ground elevation.

2.3.3 Plane Aspect

A vector was drawn to the centroid of each plane shape from the centroid of the roof shape containing that plane. The azimuthal angle of that vector was binned into a 45°-wide aspect—N, NE, E, SE, S, SW, W, or NW—indicating the side of the roof on which the plane lies. This method was found to be more reliable than determining aspect by fitting a planar surface through the subset of LiDAR points that lie above the plane's shape.

2.3.4 Shadow Rasters

The National Renewable Energy Laboratory's Solar Position and Intensity (SOLPOS) calculator [11] was used to compute hourly solar positions at the center of the study area to within ±0.01°. The Hillshade function of the GIS tool was then used to determine from solar position whether any cell in a surface elevation raster lay in shadow. For each daylight hour in the 21st day of each month (143 hours/year), a raster of "total" shading—value 1 if the cell lies in the shadow of any cell in the study region; 0 otherwise—was computed from the study-region surface-elevation raster (Fig. 4). Note that all hourly properties are instantaneous and evaluated on the hour.

A second raster of "intraparcel" shading—value 1 if the cell lies in the shadow of another cell *within its own parcel*; 0 otherwise—was generated by aggregating shadow rasters computed from the individual parcel surface-elevation rasters (Fig. 5). Intraparcel shadow rasters were computed for only 15 hours/year—the daylight subsets of 9A, 12N, 3P, and 6P LST on the 21st days of March, June, September, and December—because the time required to calculate intraparcel shading was about three orders of magnitude longer than that required to compute total shading.

Hourly "extraparcel" shadow rasters were computed by subtracting the hourly intraparcel shadow rasters from the hourly total shadow rasters (Fig. 6). Scattered values of -1 (red cells) and 1 (black cells) in the extraparcel shadow raster are artifacts of the shadow modeling process that result from small registration errors.

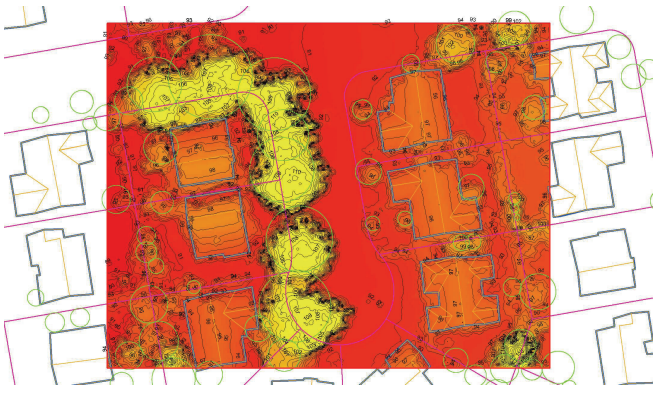

Fig. 3: Detail of surface-elevation raster (height above sea level; m).

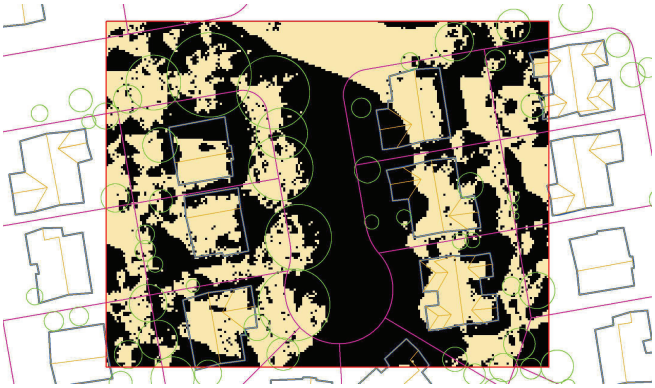

Fig. 4: Detail of total shadow raster on June 21 at 5P LST. Black cells are shaded.

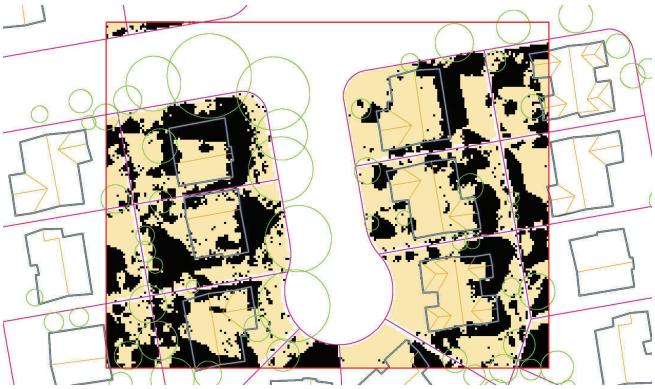

Fig. 5: Detail of intraparcel shadow raster on June 21 at 5P LST. Black cells are shaded.

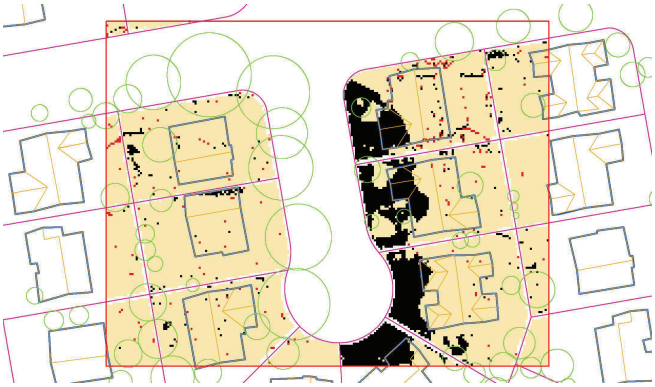

Fig. 6: Detail of extraparcel shadow raster (total shadow raster minus intraparcel shadow raster) on June 21 at 5P LST. Black cells are shaded; isolated black cells and all red cells are computational artifacts.

2.3.5 Shade Fraction and Light Loss of Each Plane

The hourly total, intraparcel, and extraparcel shade fractions of each roofing plane were computed by averaging the values of the plane's cells in the corresponding shadow raster. Hourly values of global insolation (incident osolar power/area) incident on unshaded, 5:12 pitch roofing planes in each of the eight aspects were computed with the Hay-Davies-Klutcher-Reindl radiation model [12] embedded in the California Energy Commission's CEC PV 2.3 solar calculator [13]. To reduce artifacts that can result from cloudy weather on a particular day, hourly insolations were smoothed by calculating hour-of-day running averages over an interval of -15 days to +15 days.

Total, intraparcel, and extraparcel instantaneous light losses (loss of incident solar power/area) were calculated by multiplying each hourly shade fraction by the aspect-appropriate smoothed hourly insolation.

2.3.6 Shade Fraction and Light Loss of a Set of Planes

The hourly mean shade fraction of a set of roofing planes, or fraction by which shading reduces the aggregate solar power incident on the planes at that hour, is the ratio of the planes' aggregate light loss—product of each plane's hourly shade fraction, hourly unshaded insolation, and surface area, summed over the planes—to the planes' aggregate unshaded insolation (product of each plane's hourly unshaded insolation and surface area, summed over the planes). Hourly mean total, intraparcel, and extraparcel shade fractions were computed for the subsets of roofing planes in each of the eight aspects.

The mean shade fraction F of a set of roofing planes over some time interval, or fraction by which shading reduces the aggregate solar energy incident on these planes, is the ratio of the time integral of the planes' aggregate light loss to the time integral of the planes' aggregate unshaded insolation. Monthly mean total, intraparcel, and extraparcel shade fractions for the subsets of roofing planes in each of the eight aspects were approximated by the daily mean shade fractions on the 21st day of each month. Annual mean shade fractions were evaluated by integrating over all hours of the year for which hourly shade fractions were computed.

2.3.7 Solar Access Violation

California Public Resources Code §25982 [14] states that, subject to certain exceptions,

> …no person owning, or in control of a property shall allow a tree or shrub to be placed, or, if placed, to grow on such property, subsequent to the installation of a solar collector on the property of another so as to cast a shadow greater than 10 percent of the collector absorption area upon that solar collector surface on the property of another at any one time between the hours of 10 a.m. and 2 p.m., local standard time…

The solar access of a roofing plane was considered violated in a given month if its extraparcel shade fraction exceeded 10% at any time between 10A and 2P LST on the 21st day of that month. Since extraparcel shading was calculated only at 9A, 12N, 3P, and—except in December—6P LST, extraparcel shade fractions at 10A, 11A, 1P, and 2P LST were interpolated from the calculated values.

3. RESULTS

3.1 Hourly Shading and Light Loss of SW-Facing Planes

The distribution of roofing planes by aspect was fairly uniform, with 11 – 16% of planes facing each of the eight directions. Residential rooftop solar-energy equipment is typically placed on S-, SW-, or W-facing roofing planes to maximize solar access (Table 1).

Fig. 7 charts the hourly mean total and extraparcel shade fractions and light losses for the planes that face southwest, the aspect that tends to receive the most sunlight when demand for cooling electricity peaks late in the afternoon. Values are shown in year zero and year +30 on four representative days: March 21, the spring equinox; June 21, the summer solstice, September 21, the autumn equinox; and December 21, the winter solstice.

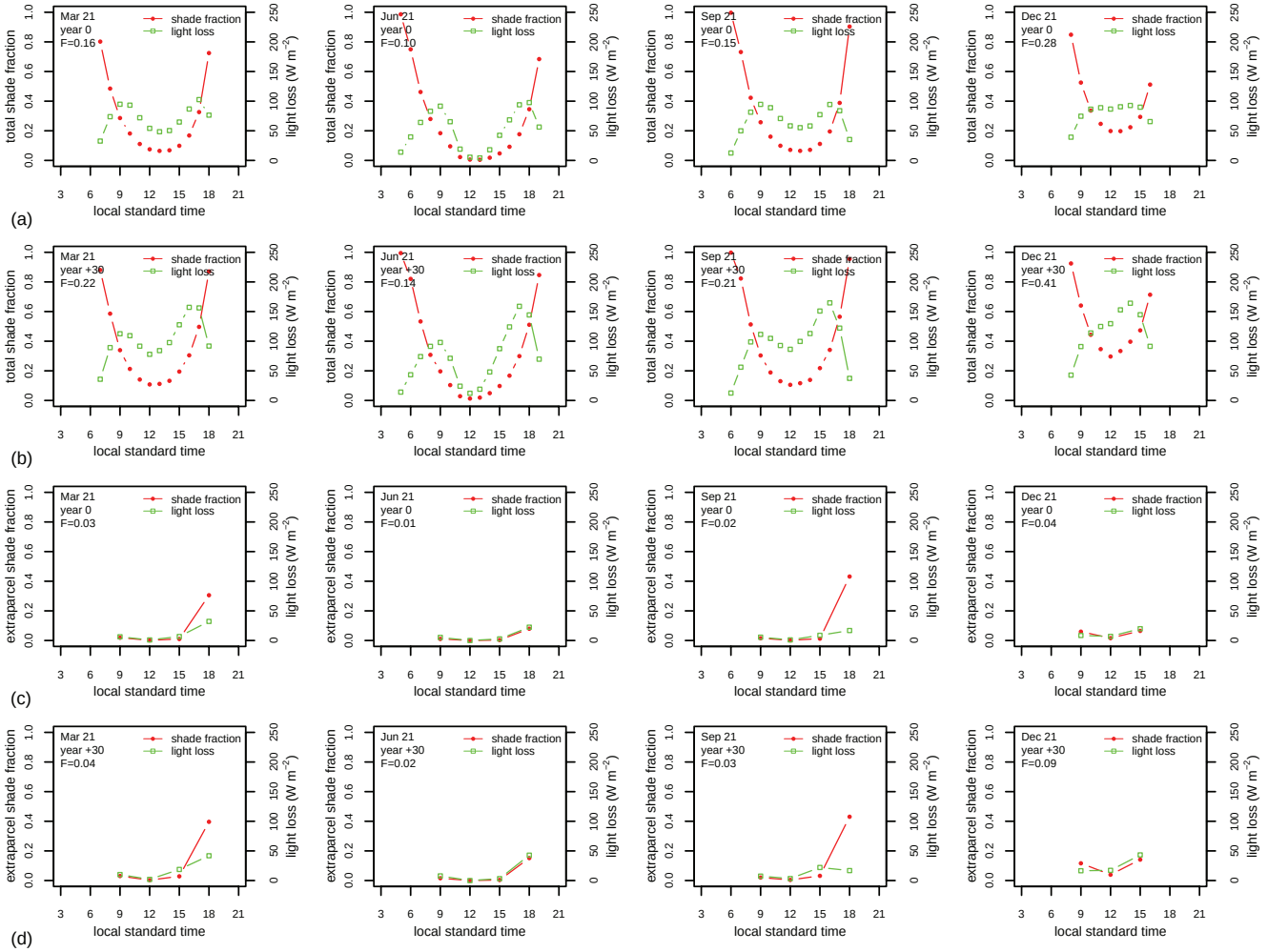

Fig. 7: Hourly shade fractions, hourly light losses, and daily shade fraction *F* for southwest-facing planes in San Jose on March 21, June 21, September 21, and December 21. Shown are (a) total shading in year zero; (b) total shading in year +30; (c) extraparcel shading in year zero; and (d) extraparcel shading in year +30.

TABLE 1: ANNUAL AND MONTHLY MEAN INSOLATIONS (W/M^2) ON AN UNSHADED, 5:12 PITCH ROOFING PLANE BY ASPECT.

	S	SW	W	NW	N	NE	E	SE
annual	233	227	204	176	159	167	192	219
Jan	129	117	90	64	51	65	93	119
Feb	206	189	151	111	91	113	154	191
Mar	242	229	198	163	146	164	199	230
Apr	272	269	251	227	212	217	238	259
May	288	297	292	275	258	250	258	273
Jun	324	331	329	317	307	301	307	316
Jul	312	318	310	292	277	272	282	298
Aug	301	300	278	248	228	231	256	283
Sep	252	243	211	174	154	165	199	234
Oct	200	187	152	112	91	107	144	181
Nov	154	141	106	70	52	68	102	137
Dec	118	107	80	53	40	52	79	106

Shadows are longest when the sun is lowest. The hourly mean total shade fraction curve on each day in each year was approximately U-shaped, with a minimum near 1P LST. In year zero, daily mean total shade fractions ranged from 0.10 in summer to 0.28 in winter (Fig. 7a). The hourly mean total shade fractions increased from year zero to year +30 as trees grew taller and their shadows grew longer. In year +30, daily mean total shade fractions ranged from 0.14 in summer to 0.41 in winter (Fig. 7b).

The shape of the hourly mean light loss curve varied seasonally and with tree growth. In year zero, spring, summer, and autumn total light losses were greatest in the mid-morning (9A LST) and late afternoon (4 – 6P LST), while winter light losses were roughly constant from mid-morning (9A LST) to mid-afternoon (3P LST) (Fig. 7a). In year +30, light losses in all seasons were about 50% higher in the late afternoon (4 – 6P LST) than in the mid-morning (9A LST) (Fig. 7b).

In both year zero and year +30, hourly mean extraparcel shade fractions were low in all seasons at 9A, 12N, and 3P LST, peaking only in response to long shadows at 6P LST. One would expect to see comparable peaks in the early morning, but the sun was below the horizon at the noon-symmetric hour of 6A LST. Hourly mean extraparcel shade fractions increased modestly from year zero to year +30. In year zero, daily mean extraparcel shade fractions ranged from 0.01 in summer to 0.04 in winter (Fig. 7c). In year +30, daily mean extraparcel shade fractions ranged from 0.02 in summer to 0.09 in winter (Fig. 7d).

3.2 Annual and Monthly Total Shade Fractions by Aspect

Table 2 and Table 3 disaggregate annual and monthly total shade fractions by plane aspect in years zero and +30, respectively. In year zero, the annual mean total shade fractions for S-, SW-, and W-facing planes ranged from 0.13 to 0.16. By year +30, the annual mean total shade fractions ranged from 0.19 to 0.23. In each year, monthly values were lowest in summer and highest in winter.

Annual and monthly extraparcel shade fractions are disaggregated by plane aspect in Table 4 (year zero) and Table 5 (year +30). In year zero, the annual mean extraparcel shade fractions for S-, SW-, and W-facing planes ranged from 0.01 to 0.02, increasing to 0.03 – 0.04 by year +30. Like those of total shading, monthly values of extraparcel shading were lowest in summer and highest in winter.

3.3 Monthly Solar Access Violations by Aspect

Solar access violations on March 21, June 21, September 21, and December 21 are disaggregated by plane aspect in Table 6 (year zero) and Table 7 (year +30). In year zero, no more than 2% of roofing planes of any aspect suffer solar access violations on June 21; by year +30, this rate still does not exceed 3%. However, the solar accesses of many S-, SW-, and W-facing roofing planes are violated in winter. In year zero, the winter violation rate was 25 – 30%; by year +30, it increased to 46 – 54%.

TABLE 2: YEAR-ZERO ANNUAL AND MONTHLY TOTAL SHADE FRACTIONS (%) OF ROOFING PLANES BY ASPECT.

	S	SW	W	NW	N	NE	E	SE
annual	13	15	16	19	19	17	16	14
Jan	22	26	29	40	43	36	30	25
Feb	17	19	22	29	32	28	24	19
Mar	13	16	18	22	24	21	18	14
Apr	10	12	13	15	16	14	13	10
May	9	10	11	12	12	11	10	9
Jun	8	10	11	11	11	10	9	8
Jul	8	10	11	12	12	11	9	8
Aug	9	11	13	15	16	14	12	10
Sep	12	15	17	22	24	20	17	14
Oct	17	20	23	31	33	28	23	19
Nov	22	25	28	40	44	36	30	25
Dec	24	28	31	44	49	40	33	27

TABLE 3: YEAR +30 ANNUAL AND MONTHLY TOTAL SHADE FRACTIONS (%) OF ROOFING PLANES BY ASPECT.

	S	SW	W	NW	N	NE	E	SE
annual	19	21	23	24	23	22	22	20
Jan	34	38	40	47	49	45	41	37
Feb	26	29	31	35	36	35	32	29
Mar	20	23	25	27	28	26	24	22
Apr	14	17	19	20	19	18	17	16
May	12	14	16	17	16	15	14	12
Jun	11	14	16	16	15	14	13	12
Jul	12	14	16	16	15	14	13	12
Aug	14	16	19	20	19	18	16	15
Sep	19	22	24	27	27	25	23	21
Oct	26	30	33	37	37	35	32	28
Nov	34	37	40	48	50	45	40	36
Dec	37	41	44	53	56	50	44	40

TABLE 4: YEAR-ZERO ANNUAL AND MONTHLY EXTRAPARCEL SHADE FRACTIONS (%) OF ROOFING PLANES BY ASPECT.

	S	SW	W	NW	N	NE	E	SE
annual	1	2	2	2	1	1	1	1
Mar	1	3	3	2	1	1	1	1
Jun	0	1	1	1	1	0	0	0
Sep	1	2	2	2	1	1	1	1
Dec	4	4	3	2	2	3	4	5

TABLE 5: YEAR +30 ANNUAL AND MONTHLY EXTRAPARCEL SHADE FRACTIONS (%) OF ROOFING PLANES BY ASPECT.

	S	SW	W	NW	N	NE	E	SE
annual	3	4	3	3	2	2	2	2
Mar	2	4	4	3	2	2	2	2
Jun	1	2	2	2	2	1	1	0
Sep	2	3	3	2	1	1	2	2
Dec	9	9	8	5	4	6	7	9

TABLE 6: YEAR-ZERO FRACTION OF ROOFING PLANES (%) IN SOLAR ACCESS VIOLATION BY MONTH AND ASPECT.

	S	SW	W	NW	N	NE	E	SE
Mar	4	6	4	2	1	4	5	8
Jun	1	2	2	1	0	1	1	1
Sep	4	6	5	1	2	3	5	7
Dec	26	30	25	15	10	18	27	32

TABLE 7: YEAR +30 FRACTION OF ROOFING PLANES (%) IN SOLAR ACCESS VIOLATION BY MONTH AND ASPECT.

	S	SW	W	NW	N	NE	E	SE
Mar	13	13	9	6	4	9	12	17
Jun	1	3	3	2	1	1	2	2
Sep	12	12	10	5	3	6	10	15
Dec	53	54	46	34	28	37	50	54

4. CONCLUSIONS

Geometric calculation of rooftop shading based on a digital elevation model of a typical residential neighborhood in San Jose, CA indicates that shadows from all sources ("total shading") reduce the annual solar access of S-, SW-, and W-facing residential roofing planes in the study area by 13 – 16%. Shadows cast by trees and buildings in neighboring parcels reduce solar access by no more than 2%. Such "extraparcel" shading violates the state-mandated solar access of no more than 7% of these planes in March, June, and September, though the violation rate is significantly higher—25 to 30%—in December.

After 30 years of simulated maximal tree growth, annual total shading increases to 19 – 22%, and annual extraparcel shading increased to 3 – 4%. The rate of solar access violation does not exceed 13% in March, June, or September, but rises to 46 – 53% in December.

Shading results for three other California cities—Sacramento, Los Angeles, and San Diego—and a fuller description of the study's methodology will be presented in a future paper.

4. ACKNOWLEDGMENTS

This work was supported by the California Energy Commission (CEC) through its Public Interest Energy Research Program (PIER), and by the Assistant Secretary for Energy Efficiency and Renewable Energy under Contract No. DE-AC02-05CH11231. We thank Bill Pennington of the California Energy Commission for helping to organize the study and for his guidance and support. We also thank the city of San Jose for providing aerial images of the study region.

5. REFERENCES

1. Kaye, R.J., R. O'Brien, N. Ghiotto and P. McKee. 1997. Site selection and assessment of rooftop photovoltaic

installations. In *Proceedings of the 14th European Photovoltaic Solar Energy Conference and Exhibition*. Barcelona, Spain; 30 June – 4 July
2. Mardaljevic, J. and M. Rylatt. 2003. Irradiation mapping of complex urban environments: an image-based approach. *Energy and Buildings* 35, 27-35
3. Compagnon, R. 2004. Solar and daylight availability in the urban fabric. *Energy and Buildings* 36, 321-328
4. CH2MHill. 2008. CH2MHill Solar Automated Feature Extraction™ Technology. Online at http://www.ch2m.com
5. Simpson, J.R. 2002. Improved estimates of tree-shade effects on residential energy use. *Energy and Buildings* 34, 1067-1076
6. Akbari, H. 2002. Shade trees reduce building energy use and CO_2 emissions from power plants. *Environmental Pollution* 116, S119-S126
7. McPherson, E.G.. and J.R Simpson. 2003. Potential energy savings in buildings by an urban tree planting programme in California. *Urban Forestry & Urban Greening* 2, 73-86
8. Akbari, H., L. S. Rose, and H. Taha. 2003. Analyzing the land cover of an urban environment using high-resolution orthophotos. *Landscape and Urban Planning* 63, 1-14
9. Rose, L.S., H. Akbari, and H. Taha. 2003. Characterizing the fabric of the urban environment: a case study of greater Houston, Texas. Lawrence Berkeley National Laboratory Report LBNL-51448, Berkeley, CA
10. ESRI. 2008. ESRI ArcView 9.1 geographic information system. Online at http://esri.com
11. NREL. 2008. National Renewable Energy Laboratory Measurement and Instrumentation Data Center (NREL MIDC) Solar Position and Intensity (SOLPOS) Calculator. Online at http://www.nrel.gov/midc/solpos/solpos.html
12. Duffie, J.A. and Beckman, W. A.. 2006. *Solar Engineering of Thermal Processes*, *3rd ed*. John Wiley & Sons
13. Wilcox, B.A. and W.A. Beckman. 2007. CEC PV Calculator 2.3. California Energy Commission. Online at http://www.gosolarcalifornia.ca.gov/nshpcalculator/download_calculator.html
14. CPRC. 2008. California Public Resources Code §25982. Online at http://www.leginfo.ca.gov/cgi-bin/displaycode?section=prc&group=25001-26000&file=25980-25986